



First-order phase transitions in the real microcanonical ensemble

Philipp Schierz,^{*} Johannes Zierenberg,[†] and Wolfhard Janke[‡]

Institut für Theoretische Physik, Universität Leipzig, Postfach 100 920, 04009 Leipzig, Germany

(Received 2 May 2016; published 9 August 2016)

We present a simulation and data analysis technique to investigate first-order phase transitions and the associated transition barriers. The simulation technique is based on the real microcanonical ensemble where the sum of kinetic and potential energy is kept constant. The method is tested for the droplet condensation-evaporation transition in a Lennard-Jones system with up to 2048 particles at fixed density, using simple Metropolis-like sampling combined with a replica-exchange scheme. Our investigation of the microcanonical ensemble properties reveals that the associated transition barrier is significantly lower than in the canonical counterpart. Along the line of investigating the microcanonical ensemble behavior, we develop a framework for general ensemble evaluations. This framework is based on a clear separation between system-related and ensemble-related properties, which can be exploited to specifically tailor artificial ensembles suitable for first-order phase transitions.

DOI: [10.1103/PhysRevE.94.021301](https://doi.org/10.1103/PhysRevE.94.021301)

First-order phase transitions are ubiquitous in nature. At the transition point two or more phases coexist, separated by highly suppressed transition states. This suppression is described by a free-energy barrier which governs the transition rate between the coexisting phases. With increasing system size, the free-energy barrier increases and the probability for a transition decreases exponentially. The result is a rapidly growing relaxation time. As a consequence, canonical Monte Carlo methods such as the Metropolis algorithm [1] fail to sample the full probability distribution, being at risk to remain stuck in a single phase. Of course, generalized-ensemble methods such as multicanonical [2,3], Wang-Landau [4], or statistical-temperature Monte Carlo [5] simulations avoid double-peak distributions and hence allow for a precise estimation of equilibrium properties. However, this comes at the cost of a sophisticated iterative procedure.

In this work, we show that replica-exchange simulations in the “real” microcanonical ensemble are a competitive and iteration free alternative to generalized-ensemble simulations at first-order phase transitions. The microcanonical ensemble itself has gained considerable interest in recent years [6–19]. One application is a complementary investigation and classification of phase transitions [10,11,17]. Not uncommonly the microcanonical ensemble is described with constant *potential* energy E_p . Considering this “conformational” microcanonical ensemble originates most likely from classical spin systems where the kinetic energy E_k is usually not defined in the Hamiltonian. Here we consider instead the real microcanonical (NVE) ensemble with constant *total* energy $E = E_k + E_p$, as discussed in any textbook on statistical mechanics. The integration of the momentum part of the microcanonical partition sum can be done analytically [9], similarly to the canonical case. Therefore the simulated phase space is reduced to the configuration part and the Metropolis scheme is straightforward to adapt. In Ref. [12], Martin-Mayor noticed that the real microcanonical ensemble is well suited to study first-order phase transitions for the q -state Potts model with

a large number of spins. We generalize this observation by applying the NVE ensemble to the test case of the droplet condensation-evaporation transition in a continuous Lennard-Jones (LJ) system [20–22]. The method is extended to replica-exchange microcanonical simulations (RE NVE) combined with the weighted histogram analysis method (WHAM) [23,24] adapted to the NVE ensemble [25–27], enabling the estimation of the density of states. Within a proposed analytical framework we discuss the advantageous sampling behavior of the NVE ensemble at temperature-driven first-order phase transitions. The developed framework is based on a generalized equal-area rule and further allows us to evaluate the behavior of physical or arbitrary ensembles for general first-order phase transitions. This framework may be used to optimize an ensemble for replica-exchange techniques.

When the momenta are integrated out, the microcanonical ensemble with fixed total energy E , particle number N , and volume V is represented by the partition function

$$\Gamma_{\text{NVE}} = C \int_{-\infty}^{\infty} dE_p \Omega(E_p) W_{\text{NVE}}(E_p), \quad (1)$$

where C is a normalization constant, $\Omega(E_p)$ is the density of states, and

$$W_{\text{NVE}}(E_p) = (E - E_p)^{\frac{3N-2}{2}} \Theta(E - E_p) \quad (2)$$

is the configuration weight with the Heaviside step function $\Theta(E - E_p)$. The Metropolis acceptance probability is then naturally adapted to the NVE ensemble:

$$P_{\text{acc}}(A \rightarrow B) = \min \left\{ 1, W_{\text{NVE}}(E_p^B) / W_{\text{NVE}}(E_p^A) \right\}. \quad (3)$$

Note that a simulation for total energy E has to start from a potential energy $E_p \leq E$ since $E_p > E$ has zero probability in this ensemble.

This can be combined with a replica-exchange scheme, where parallel simulations at different total energies exchange their configurations with the probability

$$P_{\text{exc}}(A \leftrightarrow B) = \min \left\{ 1, \frac{W_{\text{NVE}^B}(E_p^A) W_{\text{NVE}^A}(E_p^B)}{W_{\text{NVE}^B}(E_p^B) W_{\text{NVE}^A}(E_p^A)} \right\}. \quad (4)$$

Afterwards, NVE WHAM can be applied to estimate the density of states $\Omega(E_p)$. This is an ensemble-independent

^{*} philipp.schierz@itp.uni-leipzig.de

[†] johannes.zierenberg@itp.uni-leipzig.de

[‡] wolfhard.janke@itp.uni-leipzig.de

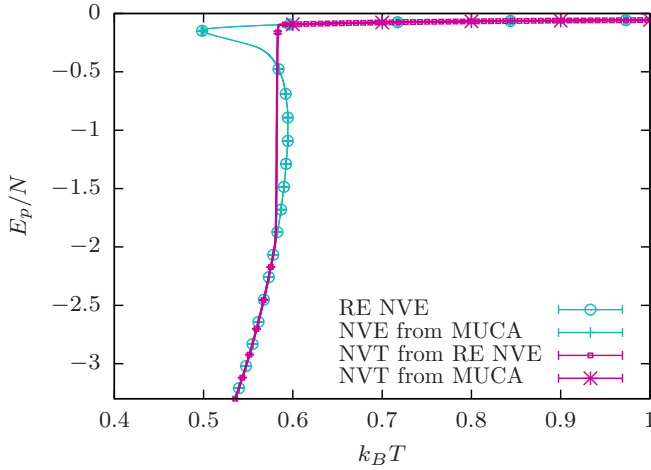


FIG. 1. Caloric curve for 512 LJ particles. Error bars are smaller than the data symbols.

property of the simulated system and allows one to estimate observables in other ensembles, e.g., the canonical NVT ensemble [25,27].

As an example for a first-order phase transition we studied droplet condensation-evaporation in a LJ system with $N \in \{384, 512, 640, 768, 1024, 2048\}$ particles at density $\rho = N/V = 0.01$. The particle-particle interaction is modeled by the LJ potential

$$U_{\text{LJ}}(r) = 4\epsilon \left[\left(\frac{\sigma}{r} \right)^{12} - \left(\frac{\sigma}{r} \right)^6 \right], \quad (5)$$

where $\epsilon = 1$ and $\sigma = 2^{-1/6}$. A cutoff was introduced at $r_c = 2.5\sigma$ with a potential shift such that $\tilde{U}_{\text{LJ}}(r) = U_{\text{LJ}}(r) - U_{\text{LJ}}(r_c)$ for $r < r_c$ and $\tilde{U}_{\text{LJ}}(r) = 0$ else. This enables the use of a domain decomposition. The RE NVE simulation with M replicas involved two simple shift moves with different update ranges. Every 20 sweeps M replicas were randomly picked to propose an exchange with a neighboring total energy replica. A sweep is here defined as N Monte Carlo steps. For each total energy we gathered a statistics of 10^6 measurements taken every second sweep after thermalization.

In a first step, we compared the NVE sampling with parallel multicanonical (MUCA) simulations [28] for 512 particles as in Ref. [22] to validate our method (see Fig. 1), where reweighting between the ensembles is performed on the level of the density of states [27]. While the temperature is a fixed parameter in the canonical ensemble, it is an observable in the microcanonical ensemble measured as $k_B T_{\text{NVE}} = 2/[(3N - 2)\langle \frac{1}{E - E_p} \rangle]$ [29]. The results are within each other's error ranges, computed by the Jackknife procedure [30].

Since both RE NVE and MUCA simulations give us a handle on the density of states, we are able to calculate the canonical probability distribution $P_{\text{NVT}}(E_p) \propto \Omega(E_p) \exp(-E_p/k_B T)$ which, as expected for a first-order phase transition, exhibits a pronounced double peak at the droplet condensation-evaporation transition (see Fig. 2). For finite systems, the transition point can be defined as the temperature T_{eqh} where the two peaks are of equal height. The potential-energy distribution in the real microcanonical

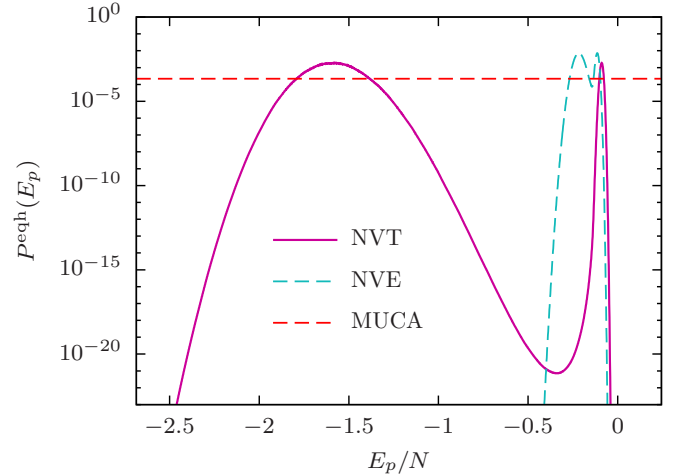


FIG. 2. NVT and NVE histograms for 2048 LJ particles at equal-height temperature $T_{\text{eqh}} = 0.6175$ and equal-height total energy $E_{\text{eqh}}/N = 0.6849$, respectively.

ensemble $P_{\text{NVE}}(E_p) \propto \Omega(E_p) W_{\text{NVE}}(E_p)$ can be either obtained directly from the NVE simulation data or from the density of states. As in the NVT ensemble, one obtains also in the NVE ensemble double-peak potential-energy histograms for certain total energies. In Fig. 2 we show the equal-height probability distribution which is realized at the transition total energy E_{eqh} . By comparing the NVT and NVE equal-height distributions we notice that the suppression in the NVE histogram is much lower than that in the NVT ensemble. This corresponds to a much lower barrier $B_{\text{NVE}} \ll B_{\text{NVT}}$, each defined by

$$B = \ln [P^{\text{eqh}}(E_p^{\pm})/P^{\text{eqh}}(E_p^0)], \quad (6)$$

where $P^{\text{eqh}}(E_p)$ is the equal-height potential-energy distribution in the respective ensemble, E_p^{\pm} refers to the location of the two maxima, and E_p^0 refers to the location of the minimum in between. Figure 3 shows the canonical and microcanonical barriers of the considered system sizes together with the

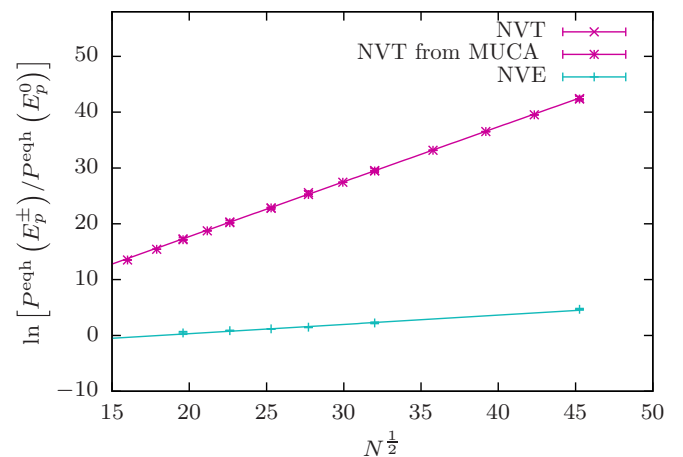


FIG. 3. The sampling barrier in the NVT and NVE ensembles, accompanying the LJ droplet condensation-evaporation transition, with a comparison to results from MUCA simulations [31].

expected leading $N^{\frac{1}{2}}$ scaling behavior according to Ref. [31] and in comparison to independent results from MUCA simulations. For the largest investigated system ($N = 2048$) we found barriers $B_{\text{NVT}} = 42.4$ and $B_{\text{NVE}} = 4.7$. This means that in the canonical ensemble the maxima of the equal-height probability distribution are 2.6×10^{18} more likely to be sampled than the minimum. This ratio is only 110 in the real microcanonical ensemble. In this manner, importance sampling in the NVE ensemble is of the order of 10^{16} times more efficient than in the canonical counterpart for this transition.

With increasing system size the barriers increase. Eventually, one reaches a point where simple Metropolis-like sampling in the NVE ensemble suffers analogous problems to the canonical counterpart. For the present example microcanonical simulations for $N = 4096$ particles were no longer feasible. Alternatively, one could apply a generalized multicanonical-like modification of RE NVE between the peaks or deploy the later discussed tailored ensembles with no barriers.

We will follow up with a detailed analytical description of the NVE sampling by giving a general picture of the sampling behavior in an arbitrary ensemble. This will give us the opportunity to arrive at conclusions about NVE barriers in comparison to NVT barriers and the barriers of arbitrary ensembles for general temperature-driven first-order phase transitions. A common approach to define a canonical transition temperature is the equal-area construction in the conformational microcanonical ensemble with fixed potential energy [7,8,10,11]:

$$\begin{aligned} B_{\text{NVT}} &= \int_{E_p^-}^{E_p^0} dE_p \left[\frac{1}{k_B T_{\text{eqa}}} - K(E_p) \right] \\ &= \int_{E_p^0}^{E_p^+} dE_p \left[K(E_p) - \frac{1}{k_B T_{\text{eqa}}} \right], \end{aligned} \quad (7)$$

where $k_B K(E_p) = \partial S / \partial E_p$ is the potential-energy derivative of the conformational microcanonical entropy $S = k_B \ln \Omega(E_p)$, being the inverse temperature in the conformational microcanonical ensemble. It is known that $K(E_p)$ shows for a first-order phase transition a typical S shape [6]. The resulting transition temperature T_{eqa} is established to be identical to the canonical equal-height temperature T_{eqh} [8]. Here we generalize this equal-area rule for an arbitrary ensemble where the configuration weight may be written as a function of the potential energy. The logarithmic probability distribution can then be expressed as

$$\ln P(E_p) = \ln \Omega(E_p) + \ln W(E_p), \quad (8)$$

where $W(E_p)$ is the probability for a configuration with potential energy E_p in a given ensemble (see Table I). Because the extrema of the distribution are the zeros of its derivative, they are trivially related to the intersection points of the derivative of the components in Eq. (8). Thus the general equal-height condition for the potential-energy distribution can be reformulated into a general equal-area rule by integrating the derivative of Eq. (8) in the ranges $[E_p^-, E_p^0]$ and $[E_p^0, E_p^+]$.

TABLE I. Configuration weights $W(E_p)$ and their (negative) logarithmic derivatives $D(E_p)$ of the canonical (NVT), microcanonical (NVE for $E_p \leq E$ [32]), multicanonical (MUCA), and multiple Gaussian modified (MGM) ensembles.

Ensemble	$W(E_p)$	$D(E_p)$
NVT	$e^{-E_p/k_B T}$	$1/k_B T$
NVE	$(E - E_p)^{\frac{3N-2}{2}}$	$(3N - 2)/2(E - E_p)$
MUCA	$\Omega(E_p)^{-1}$	$K(E_p)$
MGM	$e^{-B(A-E_p)^2}$	$-2B(A - E_p)$

Using Eq. (6), we then obtain the relation to the barrier

$$\begin{aligned} B &= \int_{E_p^-}^{E_p^0} dE_p [D(E_p) - K(E_p)] \\ &= \int_{E_p^0}^{E_p^+} dE_p [K(E_p) - D(E_p)], \end{aligned} \quad (9)$$

where the two areas are enclosed between $D(E_p) = -\ln W(E_p) / \partial E_p$, containing the ensemble dependency of the equal-area rule, and $K(E_p)$, capturing the purely system-dependent properties. In the canonical case with $D_{\text{NVT}}(E_p) = 1/k_B T$, one recovers Eq. (7).

Equation (9) provides us with an illustrative and graphical way to determine the barrier in an arbitrary ensemble. As a typical example for the S shape at a first-order phase transition we will use the $K(E_p)$ from the $N = 2048$ LJ system. For the NVT and NVE ensembles we constructed in Fig. 4 two enclosed areas of equal size by determining the specific transition temperature and transition total energy, respectively. The intersection points correspond to a minimum or maximum of $P(E_p)$ in Fig. 2. We notice that the enclosed area and hence the barrier in the NVE ensemble (turquoise blue area) is much smaller than in the NVT ensemble (hatched

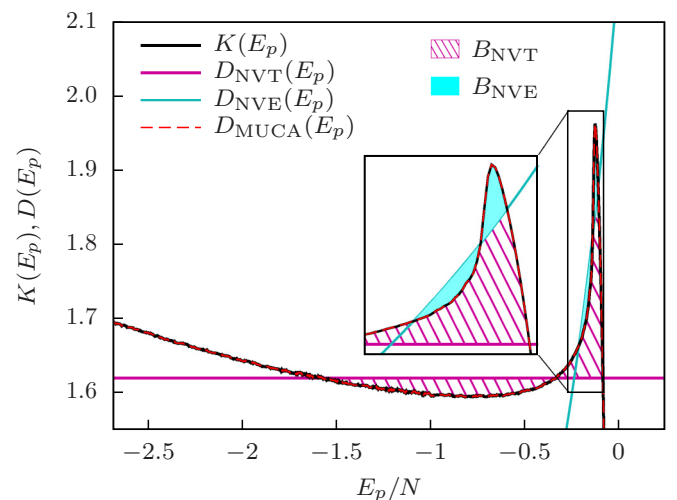


FIG. 4. The potential-energy derivative of conformational entropy $K(E_p)$ for 2048 LJ particles and the (negative) logarithmic derivative of the ensemble weights, $D_{\text{NVT}}(E_p) = 1/k_B T$ and $D_{\text{NVE}}(E_p) = (3N - 2)/2(E - E_p)$, at T_{eqh} and E_{eqh} as in Fig. 2, and $D_{\text{MUCA}}(E_p) = K(E_p)$.

magenta area). This reconfirms the observed advantage of the presented simulation technique. In general one obtains for the NVE ensemble a smaller range of transition potential energies as well as a smaller barrier than in the NVT ensemble. This is inevitable for a $K(E_p)$ with the mentioned S-shape behavior at a first-order phase transition.

The general equal-area rule allows us to arrive at further conclusions regarding earlier publications and the behavior of additional ensembles. In Ref. [27] the barrier in the NVE ensemble was observed to vanish completely in an investigation of aggregation of a polymer system. This becomes clear in the picture of the NVE equal-area rule since depending on $K(E_p)$ one might not observe three intersection points with $D_{\text{NVE}}(E_p)$ for any total energy. Therefore the barrier can vanish in the NVE ensemble which is impossible in the NVT ensemble (due to the S shape). Hence, RE NVE is identified as a good candidate for simulating aggregation transitions. In general it can be argued that an ensemble where the function $D(E_p)$ is strictly monotonically increasing has to have a smaller enclosed area than the canonical ensemble or even no enclosed area at all. Therefore any ensemble with a monotonically increasing $D(E_p)$ should show a better sampling behavior than the canonical one. It would be interesting to investigate further specific ensembles such as the Creutz demon [33].

The construction of $D(E_p)$ for an ensemble without any barrier would need, e.g., as little as a linear function with a slope larger than or equal to the largest slope of $K(E_p)$ to obtain a single intersection point and therefore avoid an enclosed area. Such a linear assumption leads directly to the multiple Gaussian modified ensemble [34] or similarly the generalized replica-exchange method [35]. A large slope, however, would cause a small width of sampled potential energies in this ensemble. The histogram width is determined by the separation between $K(E_p)$ and $D(E_p)$ around the intersection point E_p^i due to

$$\ln \left(\frac{P(E_p)}{P(E_p^i)} \right) = \int_{E_p^i}^{E_p} dE'_p [D(E'_p) - K(E'_p)] \quad (10)$$

and is often dominated by the intersection angle of these functions. The different histogram widths are also observed for the canonical left-hand-side and right-hand-side peaks in Fig. 2 since they correspond to the different intersection angles of $D_{\text{NVT}}(E_p)$ with $K(E_p)$ in Fig. 4. For the linear $D(E_p)$ the controllable width for different replicas then allows control over the amount of sampling for separate potential-energy regions. In this manner one could tailor an ensemble for an enhanced sampling in the phase-crossing region to increase tunneling events between the phases. With this reasoning it becomes clear that, e.g., the multiple Gaussian modified ensemble needs a careful determination of the optimal slope and offset parameters. One might also consider other nonlinear forms for $D(E_p)$ which may be used to determine the complete shape of the potential-energy histogram according to Eq. (8).

Alternatively, generalized ensemble simulations such as MUCA and Wang-Landau avoid barriers (or enclosed areas) by $D(E_p) = K(E_p)$. In this manner flat-histogram methods are of course the best way to sample the complete potential-energy region, however, at the cost of a computationally expensive iterative estimate of $K(E_p)$. In comparison, RE

NVE has the advantage that it just requires an appropriate choice of the total energies used in the replica-exchange Metropolis sampling. Therefore it has an advantage in terms of the parameter number to the multiple Gaussian modified ensemble and an implementation-time and simulation-time advantage to MUCA and Wang-Landau simulations due to the absence of the iteration procedure. It is remarkable that the presented NVE versus NVT barrier difference is a physical one and not restricted to computational considerations. Physical microcanonical signatures might be approximately observed in astrophysics or extremely isolated systems on earth where the barrier difference should show up as well.

The presented analytical framework and the conclusions about barrier reductions are not restricted to ensembles at constant volume and particle number. The framework may be formulated equivalently to deduce a barrier reduction for the comparison of the grandcanonical (μ VT) and its microcanonical-like counterpart, the μ VL ensemble with constant $L = E - \mu N$ [25]. Yet another possibility is a barrier reduction between the barostatic-isothermal (NPT) and isobaric-isoenthalpic (NPH) ensemble [25] for which we observed the expected barrier reduction in preliminary tests. A modified framework may also be used to tailor configuration weights to avoid barriers in field-driven phase transitions. Here one would have to start, e.g., from the magnetization double-peak distribution to derive the modified framework.

We conclude that the NVE sampling method is a powerful tool for the investigation of a wide spectrum of first-order phase transitions, as demonstrated on the example of LJ droplet formation. Systems with strong canonical first-order phase transitions show in the microcanonical ensemble only a weaker first-order or even crossover signal [12,27]. As a consequence this enables one to efficiently apply replica-exchange methods similar to the original formulation of parallel tempering. This simple technique yields an estimate of the density of states with multihistogram reweighting and gives direct access to canonical free-energy barriers and the associated transition rates. Equivalently, one could apply the same framework to energy-conserving molecular dynamics simulations since they are closely related to the NVE ensemble [9,27,36]. Considering the NVE ensemble has thus potential applications for molecular dynamics and Monte Carlo simulations estimating free-energy barriers at first-order phase transitions. The here presented framework allowed us to compare the sampling in the canonical ensemble, microcanonical ensemble, multicanonical ensemble, and the multiple Gaussian modified ensemble. Additionally, it bears the potential to construct perfectly tailored ensembles for the investigation of first-order phase transitions.

This project was funded by the European Union and the Free State of Saxony through the ESF Junior Research Group No. 241 202, the Deutsche Forschungsgemeinschaft (DFG) under Grant No. JA 483/31-1, the Leipzig Graduate School of Natural Sciences “BuildMoNa,” and the Deutsch-Französische Hochschule (DFH-UFA) under Grant No. CDFA-02-07 through the Doctoral College “L⁴”. For the provided computing time we thank the John von Neumann Institute for Computing (NIC), which gave us access to the supercomputer JURECA at Jülich Supercomputing Centre (JSC) under Grant No. HLZ24.

- [1] N. Metropolis, A. W. Rosenbluth, M. N. Rosenbluth, A. H. Teller, and E. Teller, *J. Chem. Phys.* **21**, 1087 (1953).
- [2] B. A. Berg and T. Neuhaus, *Phys. Lett. B* **267**, 249 (1991); *Phys. Rev. Lett.* **68**, 9 (1992).
- [3] W. Janke, *Int. J. Mod. Phys. C* **03**, 1137 (1992); *Physica A* **254**, 164 (1998).
- [4] F. Wang and D. P. Landau, *Phys. Rev. Lett.* **86**, 2050 (2001); *Phys. Rev. E* **64**, 056101 (2001).
- [5] J. G. Kim, J. E. Straub, and T. Keyes, *Phys. Rev. Lett.* **97**, 050601 (2006).
- [6] A. Hüller, *Z. Phys. B* **93**, 401 (1994).
- [7] M. Hao and H. A. Scheraga, *J. Phys. Chem.* **98**, 4940 (1994).
- [8] W. Janke, *Nucl. Phys. B* **63**, 631 (1998).
- [9] F. Calvo, J. P. Neirotti, D. L. Freeman, and J. D. Doll, *J. Chem. Phys.* **112**, 10350 (2000).
- [10] D. H. E. Gross, *Microcanonical Thermodynamics: Phase Transitions in “Small” Systems* (World Scientific, Singapore, 2001).
- [11] C. Junghans, M. Bachmann, and W. Janke, *Phys. Rev. Lett.* **97**, 218103 (2006); *J. Chem. Phys.* **128**, 085103 (2008).
- [12] V. Martin-Mayor, *Phys. Rev. Lett.* **98**, 137207 (2007).
- [13] M. Kastner and M. Pleimling, *Phys. Rev. Lett.* **102**, 240604 (2009).
- [14] T. Chen, L. Wang, X. Lin, Y. Liu, and H. Liang, *J. Chem. Phys.* **130**, 244905 (2009).
- [15] M. P. Taylor, W. Paul, and K. Binder, *J. Chem. Phys.* **131**, 114907 (2009).
- [16] M. Möddel, W. Janke, and M. Bachmann, *Phys. Chem. Chem. Phys.* **12**, 11548 (2010).
- [17] S. Schnabel, D. T. Seaton, D. P. Landau, and M. Bachmann, *Phys. Rev. E* **84**, 011127 (2011).
- [18] J. Zierenberg and W. Janke, *Europhys. Lett.* **109**, 28002 (2015).
- [19] M. Marenz and W. Janke, *Phys. Rev. Lett.* **116**, 128301 (2016).
- [20] L. G. MacDowell, P. Virnau, M. Müller, and K. Binder, *J. Chem. Phys.* **120**, 5293 (2004).
- [21] M. Schrader, P. Virnau, and K. Binder, *Phys. Rev. E* **79**, 061104 (2009).
- [22] J. Zierenberg and W. Janke, *Phys. Rev. E* **92**, 012134 (2015).
- [23] A. M. Ferrenberg and R. H. Swendsen, *Phys. Rev. Lett.* **63**, 1195 (1989).
- [24] S. Kumar, J. M. Rosenberg, D. Bouzida, R. H. Swendsen, and P. A. Kollman, *J. Comput. Chem.* **13**, 1011 (1992).
- [25] F. A. Escobedo, *Phys. Rev. E* **73**, 056701 (2006).
- [26] J. Kim, T. Keyes, and J. E. Straub, *J. Chem. Phys.* **135**, 061103 (2011).
- [27] P. Schierz, J. Zierenberg, and W. Janke, *J. Chem. Phys.* **143**, 134114 (2015).
- [28] J. Zierenberg, M. Marenz, and W. Janke, *Comput. Phys. Commun.* **184**, 1155 (2013).
- [29] E. M. Pearson, T. Halicioglu, and W. A. Tiller, *Phys. Rev. A* **32**, 3030 (1985).
- [30] B. Efron, *The Jackknife, the Bootstrap, and Other Resampling Plans* (Society for Industrial and Applied Mathematics, Philadelphia, PA, 1982).
- [31] J. Zierenberg, P. Schierz, and W. Janke, [arXiv:1607.08355](https://arxiv.org/abs/1607.08355) (2016).
- [32] Please note that the domain of the function $D_{\text{NVE}}(E_p)$ is limited to $[-\infty, E]$ since the logarithmic derivative of $W(E_p)$ is only defined within these boundaries.
- [33] M. Creutz, *Phys. Rev. Lett.* **50**, 1411 (1983).
- [34] T. Neuhaus and J. S. Hager, *Phys. Rev. E* **74**, 036702 (2006).
- [35] J. Kim, T. Keyes, and J. E. Straub, *J. Chem. Phys.* **132**, 224107 (2010).
- [36] R. Lustig, *J. Chem. Phys.* **100**, 3048 (1994).